Schizophrenia Bulletin vol. 41 no. 2 pp. 471–482, 2015
doi:10.1093/schbul/sbu078
Advance Access publication June 9, 2014

Detecting the Psychosis Prodrome Across High-Risk Populations Using Neuroanatomical Biomarkers

Nikolaos Koutsouleris*[,1], Anita Riecher-Rössler[2,4], Eva M. Meisenzahl[1], Renata Smieskova[2], Erich Studerus[2], Lana Kambeitz-Ilankovic[1], Sebastian von Saldern[1], Carlos Cabral[1], Maximilian Reiser[3], Peter Falkai[1], and Stefan Borgwardt[2]

[1]Department of Psychiatry and Psychotherapy, Ludwig-Maximilian-University, Munich, Germany; [2]Department of Psychiatry, University of Basel, Basel, Switzerland; [3]Department of Radiology, Ludwig-Maximilian-University, Munich, Germany

[4]This author contributed equally to this article.

*To whom correspondence should be addressed; Department of Psychiatry and Psychotherapy, Ludwig-Maximilian-University, Nussbaumstr. 7, 80336 Munich, Germany; tel: +49-89-4400-55885, fax: +49-89-4400-55776, e-mail: nikolaos.koutsouleris@med.uni-muenchen.de

To date, the MRI-based individualized prediction of psychosis has only been demonstrated in single-site studies. It remains unclear if MRI biomarkers generalize across different centers and MR scanners and represent accurate surrogates of the risk for developing this devastating illness. Therefore, we assessed whether a MRI-based prediction system identified patients with a later disease transition among 73 clinically defined high-risk persons recruited at two different early recognition centers. Prognostic performance was measured using cross-validation, independent test validation, and Kaplan-Meier survival analysis. Transition outcomes were correctly predicted in 80% of test cases (sensitivity: 76%, specificity: 85%, positive likelihood ratio: 5.1). Thus, given a 54-month transition risk of 45% across both centers, MRI-based predictors provided a 36%-increase of prognostic certainty. After stratifying individuals into low-, intermediate-, and high-risk groups using the predictor's decision score, the high- vs low-risk groups had median psychosis-free survival times of 5 vs 51 months and transition rates of 88% vs 8%. The predictor's decision function involved gray matter volume alterations in prefrontal, perisylvian, and subcortical structures. Our results support the existence of a cross-center neuroanatomical signature of emerging psychosis enabling individualized risk staging across different high-risk populations. Supplementary results revealed that (1) potentially confounding between-site differences were effectively mitigated using statistical correction methods, and (2) the detection of the prodromal signature considerably depended on the available sample sizes. These observations pave the way for future multicenter studies, which may ultimately facilitate the neurobiological refinement of risk criteria and personalized preventive therapies based on individualized risk profiling tools.

Key words: neuroanatomical biomarker/individualized risk stratification/cross-center/machine learning

Introduction

Two decades of early recognition research revealed that patterns of subtle prodromal symptoms allow persons with at-risk mental states (ARMS) for psychoses to be reliably identified using clinical high-risk criteria. Compared to the general population, these persons have a 100-fold higher risk for developing these devastating mental illnesses. However, relying solely on these symptoms leads to a correct 24-month disease prediction in only 29%[1] of cases and a 10-year transition likelihood between 35%[2] and 49%.[3] Therefore, tailoring preventive treatment to each individual's risk while minimizing harmful medication effects requires these rates to be considerably improved using valid and accessible prognostic markers.

An array of candidate biomarkers has been recently identified, suggesting that the ARMS is associated with alterations of neurocognitive performance[4] and brain abnormalities at the neuroanatomical,[5] functional,[6–8] and chemical[9,10] levels. Overall, these alterations seem to be similar to, but less severe than those in the established disease.[11] More specifically, structural imaging studies comparing ARMS individuals with a subsequent full-blown illness (ARMS-T) to those without a later disease transition (ARMS-NT) showed reduced gray matter (GM) in prefrontal, temporal, cingulate, insular, and subcortical brain structures in the former vs the latter group.[12] However, most of these structural differences—albeit significant at the group level—have so far failed to produce clinically viable markers of the psychosis prodrome.

The gap between this research and its desired clinical application may originate from current study designs and univariate analysis methods: (1) vulnerability for reporting bias due to the small-sample problem inherent in monocentric high-risk research,[13] (2) decomposition of complex psychosis-related brain patterns into single voxels or clusters,[14] and hence (3) severe limitations in tracing these patterns in individuals as these univariate projections are quantified in terms of *group-level statistical significance*. Unfortunately, significance is largely useless for guiding the diagnostic process because a biomarker's applicability rather depends on its sensitivity and specificity, which measure its predictive performance at the *single-subject level*.[15]

In contrast, multivariate pattern recognition methods, such as support vector machines (SVM),[16] have recently emerged as promising tools for the individualized diagnosis of various neuropsychiatric conditions[17,18] based on their capacity to "learn" the innate interregional dependencies of distributed brain pathologies from training data and generalize the learned discriminative rules to new, unseen patients.[19] Thus, these methods may promote an objective way to increase prognostic certainty to levels required for individualized prevention, as shown by our previous work in two independent ARMS samples from Munich and Basel.[20,21]

Although these initial results support the utility of neuroimaging in predicting psychosis, tough replication and verification of these initial candidate markers is needed according to current biomarker development regulations.[22] A crucial validation step within this translational process is the demonstration of individualized disease prediction based on a single neuroanatomical signature evidenced *across* independent ARMS cohorts. The identification of such a cross-center signature is challenged by the clinical, neurobiological, and MRI-related heterogeneity of current small-sample ARMS cohorts. Hence, our previous findings potentially resulted from an accidentally good separability of our single-center study populations.[20,21]

This study is to our knowledge the first and to date largest study on the MRI-based cross-center prediction of psychosis. We hypothesized that the underlying biomarker would consist of a pattern of prefrontal, temporal, and subcortical brain alterations enabling the classification of true vs false prodromal individuals *across* independent ARMS populations. Furthermore, we expected the "neuroanatomical risk" computed from an ARMS person's loading on this signature to be closely related to their psychosis risk, as measured in terms of psychosis-free survival time.

Materials and Methods

Participants

We examined a pooled database of 73 ARMS individuals, who were previously enrolled into prospective, naturalistic studies conducted independently at the Early Recognition Services of the Department of Psychiatry and Psychotherapy ("Früherkennungs- und Therapiezentrum," FETZ), Ludwig-Maximilian-University, Munich, Germany, and the Department of Psychiatry ("Früherkennung von Psychosen," *FePsy*), University of Basel, Switzerland. Detailed study descriptions were given in earlier work.[21,23] In summary, both sites employed clinical ultra-high-risk criteria closely corresponding to the well-established Personal Assessment and Crisis Evaluation (PACE) definitions.[15–17] At the FETZ, cognitive-perceptual basic symptoms additionally defined psychosis risk:[3] Hence, ARMS inclusion required (*a*) basic symptoms (FETZ), and/or (*b*) Attenuated Positive Symptoms (FETZ and *FePsy*), and/or (*c*) Brief Limited Intermittent Psychotic Symptoms (FETZ and *FePsy*) fulfilling specific time criteria, or (*d*) Decline in global functioning combined with risk-conferring traits as defined by each center's intake criteria (Supplementary Methods). Additionally, prodromal symptoms were assessed with the Brief Psychiatric Rating Scale (BPRS) and Scale for the Assessment of Negative Symptoms (SANS; Basel) and with the Positive and Negative Symptoms Scale (PANSS; Munich).

Exclusion criteria were age < 18 years, insufficient knowledge of German, IQ < 70, previously diagnosed psychotic disorders or transient psychotic episodes meeting transition criteria (see below), a diagnosed brain disease or substance dependency (except for cannabis in *FePsy*), previous head traumas, neurological, serious medical or surgical illnesses, or lifetime diagnoses of psychotic or borderline personality disorders as assessed by an experienced psychiatrist in detailed clinical interviews. Prior to study inclusion, only 4 out of 73 ARMS individuals had received low doses of atypical antipsychotics for behavioral control by the referring psychiatrist or general practitioner (3 participants olanzapine, 1 risperidone), all for less than 3 weeks.

All subjects were regularly followed over 4 years and were offered supportive counseling and clinical management. At both centers, transition criteria were monitored monthly in the first year and quarterly thereafter using BPRS/PANSS severity thresholds closely corresponding to refs.[24,25]: hallucinations scores ≥4 on the respective BPRS or PANSS item; OR scores ≥5 on the unusual though content or suspiciousness (BPRS)/delusions (PANSS) item, or on the conceptual disorganization item of either scale. Symptoms had to occur daily and persist for >1 week to be deemed a transition to frank psychosis. Using these criteria, the ARMS group was subdivided into 40 nontransitions (ARMS-NT) and 33 transitions (ARMS-T, transition rate: 45.2%; 95%-CI: 33.5%–56.9%). The mean (median; SD) follow-up period in the ARMS-NT group was 4.3 years (4.4; 1.5). In both centers, a diagnosis of first-episode psychosis was corroborated 1 year after transition using the

Diagnostic and Statistical Manual of Mental Disorders, Fourth Edition (DSM-IV) criteria in Munich and the OPCRIT (Operational Criteria Checklist for Psychotic and Affective Illness)[26] in Basel. Diagnostic criteria for schizophrenia/schizoaffective disorder were met by 22/5 transitions. OPRCRIT diagnoses were unavailable for 6 ARMS-T subjects, which could not be contacted. To build the MRI predictor, we selected 33 ARMS-NT individuals to match the ARMS-T group with respect to age, gender, and education years (table 1). The data of the remaining 7 subjects were used to further validate the MRI predictor after training and cross-validation.

All aspects of the study were reviewed and approved by the local ethics committees of both universities. Written informed consent was obtained from each participant before study inclusion.

MRI Data Acquisition and Preprocessing

MRI data acquisition and preprocessing were described in previous work[21,27,28] and are also detailed in the Supplementary Methods. All images were first carefully checked for MRI scanner artifacts and gross anatomical abnormalities by trained clinical neuroradiologists and then processed using the VBM8 toolbox (http://dbm.neuro.uni-jena.de/vbm8/). This preprocessing produced modulated and normalized GM segments, which were smoothed with a 4 mm full-width-at-half-maximum Gaussian kernel prior to the subsequent analysis steps.

Multivariate Pattern Classification Analysis

We used our pattern recognition tool NeuroMiner to implement a fully automated machine learning pipeline, which (1) constructed sets of predictive neuroanatomical features from high-dimensional GM maps, and (2) learned decision rules from these features to predict psychosis at the single-subject level. To strictly separate the training process from the evaluation of the predictor's generalization capacity, the pipeline was completely embedded into a repeated, double cross-validation framework[29] (rdCV). As described previously,[27] rdCV computes an *unbiased* estimate of the method's expected diagnostic accuracy on new cases, rather than merely fitting the current study population. Furthermore, rdCV produces *predictor ensembles* that optimally separate single individuals from different groups, while avoiding overfitting to the peculiarities of the training data.

More specifically, the following analysis steps were wrapped into a Leave-One-Per-Group-Out cross-validation cycle at the outer (CV_2) and the inner (CV_1) cycles of rdCV: each training sample's GM tissue maps were initially corrected for center effects using partial correlation analysis and scaled voxel-wise to the range [0,1]. These maps entered a multivariate local linear learning algorithm[30] that weighted voxels according to the geometric distance ("margin") they conjointly induced between the ARMS-NT and ARMS-T classes. The algorithm's parameters were a priori set to $\sigma = 2$ and $\lambda = 0.5$ to extract *sparse*, nonredundant voxel sets from the data. To further reduce feature dimensionality, subsets of correlated voxels within the extracted patterns were projected to uncorrelated principal components (PC) using Robust Principal Component Analysis.[31] These PC features entered a linear ν-SVM algorithm (LIBSVM, (http://www.csie.ntu.edu.tw/~cjlin/libsvm/) that determined the optimal between-group boundary by maximizing the margin between the neuroanatomically most similar subjects of opposite groups (the "support vectors").[32] Optimal PC number and ν parameters were determined for each training sample within the inner rdCV cycle.

Finally, unseen CV_1 and CV_2 test subjects were processed by successively applying all training parameters to the test data: adjustment for center effects (partial correlations), voxel-wise scaling and weighting, dimensionality reduction, and linear kernel projection. Within kernel space, the SVM classifier determined a test subject's geometric position relative to the learned decision boundary, resulting in a decision value and a group membership prediction. This analysis sequence was repeated for each CV_1 training partition in a given CV_2 training fold, thus generating an ensemble classifier which computed a CV_2 test subject's group membership by averaging the decision scores of its SVM base learners (Supplementary Methods). Finally, for each subject, ensemble decisions were aggregated across those partitions, in which this subject had not been involved in the training process. Majority voting was used to determine the test subject's *class probability*, and thus its final out-of-training (OOT) group membership. Moreover, we applied the trained prediction system to the MRI data of the 7 ARMS-NT individuals, who were initially removed from the database. The predictive signature was visualized by computing the average voxel probability map across the entire rdCV structure as described in refs.[20,27] (figure 1). Moreover, a parcellation analysis (table 3) measured the distribution of reliably predictive voxels across the 116 brain regions of the AAL template (Automated Anatomical Labeling).[33,34]

Two additional analyses were carried out using the same parameter setup as described above (Supplementary Results): In Supplementary Analysis 1 we quantified the strength of between-center effects comprising MRI and population-related differences, as well as the capacity of our correction method to mitigate these effects. Supplementary Analysis 2 measured how an ARMS-T sample size reduction in two-, four-, and six-out experiments affected OOT predictions and generalization to the independent test sample, extended by the left-out subjects.

Finally, a Kaplan-Meier survival analysis was performed in the entire ARMS population to assess the time dependency of transition with respect to neuroanatomical risk as defined by the subjects' decision scores. Therefore, the cohort's

Table 1. Sociodemographic and Clinical Characteristics of the Study Groups

	Basel			Munich				Pooled Data			Test Data
	ARMS-T	ARMS-NT	*P*	ARMS-T	ARMT-NT	*P*	*Pc*	ARMS-T	ARMS-NT	*P*	ARMS-NT
Sociodemographic variables											
N	16	16		17	17			33	33		7
Mean age at baseline [y] (SD)	26.4 (6.5)	24.6 (6.4)	ns	23.6 (4.6)	24.6 (5.4)	ns	ns	25.0 (5.7)	24.6 (5.8)	ns	24.7 (8.7)
Sex (male)	11 (69%)	10 (63%)	ns	13 (77%)	10 (59%)	ns	ns	24 (73%)	20 (61%)	ns	3 (43%)
Handedness (mixed or left)	3 (19%)	0 (0%)	ns	0 (0%)	4 (24%)	ns	ns	3 (9%)	4 (12%)	ns	1 (14%)
Educational level											
<9 y	5 (31%)	4 (25%)	ns	0 (0%)	0 (0%)	ns	ns	4 (12%)	5 (15%)	ns	0 (0%)
9–11 y	5 (31%)	6 (38%)		5 (29%)	9 (52%)			11 (33%)	14 (42%)		2 (29%)
12–13 y	3 (19%)	5 (31%)		12 (70%)	8 (47%)			17 (52%)	11 (33%)		3 (43%)
>13 y	3 (19%)	1 (6%)		0 (0%)	0 (0%)			1 (3%)	3 (9%)		2 (29%)
Mean verbal IQ [MWT-B] (SD)	110.3 (12.8)	112.9 (13.4)	ns	104.2 (17.2)	109.4 (14.1)	ns	ns	107.6 (14.9)	111.1 (13.7)	ns	101.5 (17.8)
Clinical variables											
Individuals with a first-degree relative with schizophrenia	2 (13%)	3 (19%)	ns	5 (29%)	1 (6%)	ns	ns	7 (22%)	4 (12%)	ns	3 (43%)
Mean BPRS global score at intake (SD)	41.9 (10.6)	36.4 (6.9)	ns	—	—	—	—	—	—	—	39.8 (8.1)
Mean PANSS total score at intake (SD)	—	—	—	61.3 (22.5)	47.9 (9.3)	ns	—	—	—	—	41.5 (3.5)
Mean SANS at intake (SD)	9.5 (5.4)	6.6 (4.8)	ns	—	—	—	—	—	—	—	7.6 (3.6)
Mean MADRS score at intake (SD)	—	—	—	17.3 (6.9)	12.8 (9.1)	ns	—	—	—	—	17.0 (5.2)
Mean BPRS depression + anxiety score at intake (SD)	9.3 (3.4)	7.9 (9.3)	ns	—	—	—	—	—	—	—	8.0 (1.9)
Mean/median interval between baseline MRI scan and disease transition [mo] (SD; range)	13.5/10.1 (15.3; 55.1)	—	—	5.8/2.7 (7.4; 24.7)	—	—	ns	9.7/3.8 (12.4; 55.1)	—	—	—

Note: ARMS-T: high-risk persons with a subsequent transition to psychosis; ARMS-NT: high-risk persons without a subsequent transition to psychosis; MWT-B: Mehrfach-Wortschatztest B; BPRS: Brief Psychiatric Rating Scale; PANSS: Positive and Negative Symptom Scale; SANS: Scale for the Assessment of Negative Symptoms; MADRS: Montgomery-Asberg Depression Rating Scale; MRI: magnetic resonance imaging. Descriptive analyses and statistical test results are shown for within-center and pooled data analyses (chi-square tests were applied to sex, handedness, educational level, and individuals with a first-degree relative with schizophrenia. All other variables were evaluated using *t* tests, *P* significance). Furthermore, two-way analyses were carried out to evaluate possible center × group interaction effects (categorical data: chi-square tests, continuous data: *t* tests, *P* significance).

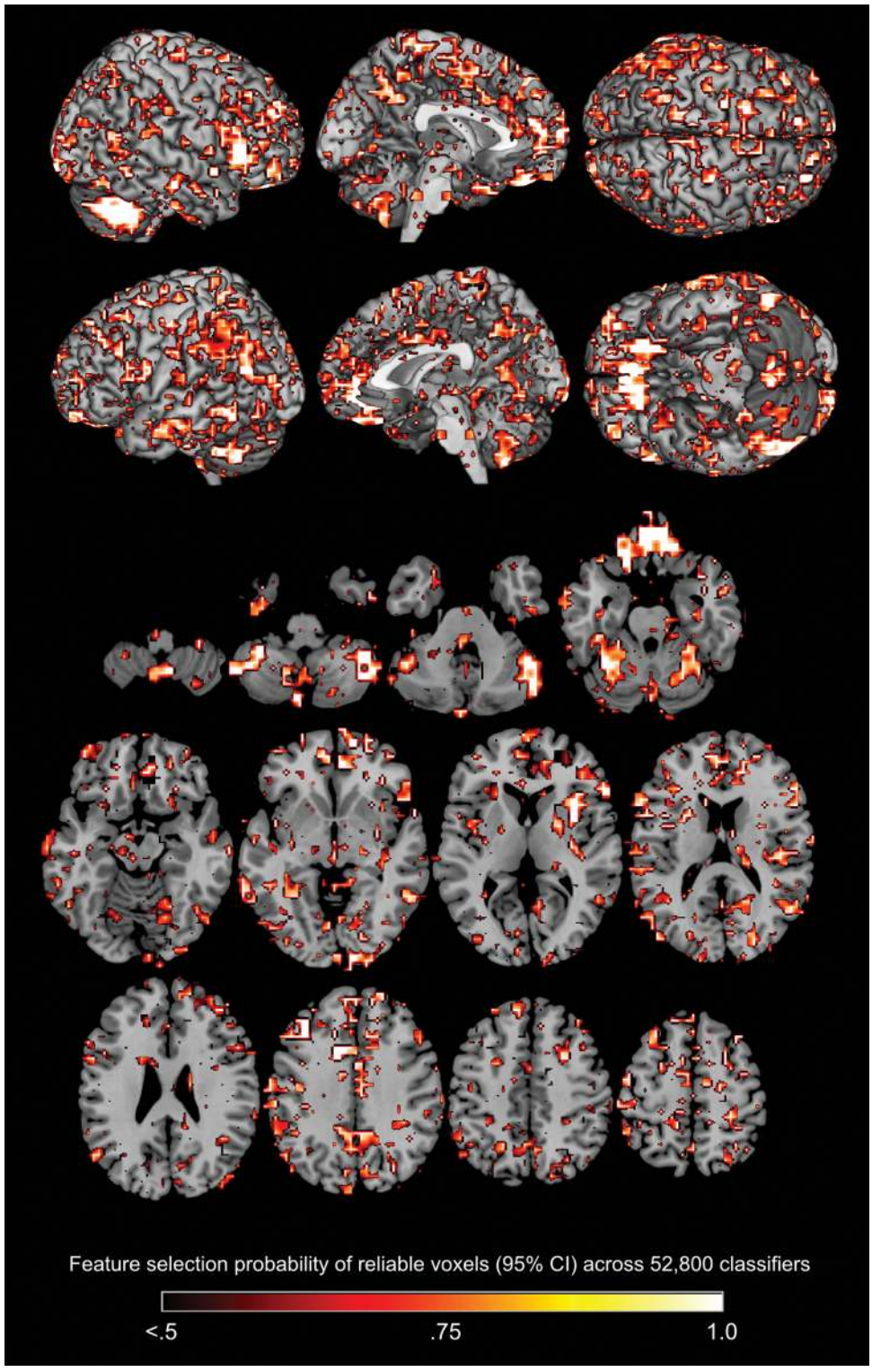

Fig. 1. Voxel probability map of reliable contributions to the ARMS-NT vs ARMS-T decision boundary. Voxels with a probability of >50% were overlaid on the single subject Montreal Neurological Institute template using the MRIcron software package (http://www.sph.sc.edu/comd/rorden/mricron/). ARMS, at-risk mental states.

decision values were split into 33%-quantiles that assigned subjects to "low," "intermediate," and "high-risk" levels. Median survival times, transition rates, and recruitment center compositions were compared between risk levels using median and chi-square tests. Pairwise differences between survival functions were evaluated using log-rank tests.

Results

Sociodemographic and Clinical Findings

No significant center effects were found between the Basel and Munich samples regarding transition rates (Basel: 43.2%, Munich: 47.2%) and MRI-to-psychosis intervals (table 1). Furthermore no center × group effects were found for age, sex, handedness, educational level, verbal IQ, family history of psychosis in first-degree relatives. Within each center, ARMS-T and ARMS-NT groups did not differ in these parameters, as well as regarding prodromal and depressive symptoms (table 1).

SVM Classification Analysis

In the pooled dataset ($N = 66$) the MRI predictor correctly classified ARMS-T and ARMS-NT individuals with an OOT accuracy of 80.3% (sensitivity = 75.8% / specificity = 84.8%, table 2). Only 1 of 7 independent ARMS-NT persons was wrongly labeled as ARMS-T (specificity = 85.7%, false positive rate = 14.3%). Thus, the generalization performance in the entire database ($N = 73$) attained a balanced accuracy of 80.4% (75.8% / 85%). Given a pretest disease probability of 45.2%, the positive / negative likelihood ratios of 5.1 / 0.29 indicate that an ARMS person with a positive / negative MRI finding would have an posttest probability of 81% / 19% for developing psychosis. The MRI predictor's diagnostic odds ratio in the entire database measured 17.7. Finally, the Kaplan-Meier analysis (figure 2, table 3) detected a nonlinear accumulation of risk in the upper 33%-quantile of the neuroanatomical decision scores. This risk accumulation consisted of a nonlinear survival time decrease and transition rate increase from the low- to the high-risk groups: high-risk

Table 2. Prediction Performance

Dataset	TP	TN	FP	FN	Sens [%]	Spec [%]	BAC [%]	FPR [%]	PPV [%]	NPV [%]	LR+	LR−	DOR	Pre	Post
Pooled	25	28	5	8	75.8	84.8	80.3	15.2	83.3	77.8	5.00	0.29	17.3		
Basel	11	13	3	5	68.8	81.3	75.0	18.8	78.6	72.2	3.67	0.38	9.5		
Munich	14	15	2	3	82.4	88.2	85.3	11.8	87.5	83.3	7.00	0.20	35		
Test	0	6	1	0		85.7		14.3		100.0					
Overall	25	34	6	8	75.8	85.0	80.4	15.0	80.6	81.0	5.05	0.29	17.7	45.2	81.0

Note: The performance of the MRI prediction system was evaluated by means of sensitivity (Sens), specificity (Spec), balanced accuracy (BAC), false positive rate (FPR), positive / negative predictive value (PPV/NPV) as well as positive/negative likelihood and diagnostic odds ratio (LR+/LR−, DOR). These measures were calculated from the confusion matrix containing the number of true positives (TP), false negatives (FN), true negatives (TN), and false positives (FP). Furthermore, the posttest probability of developing psychosis (Post) after having a positive MRI testing was computed based on LR+ and the pretest probability (=transition rate).

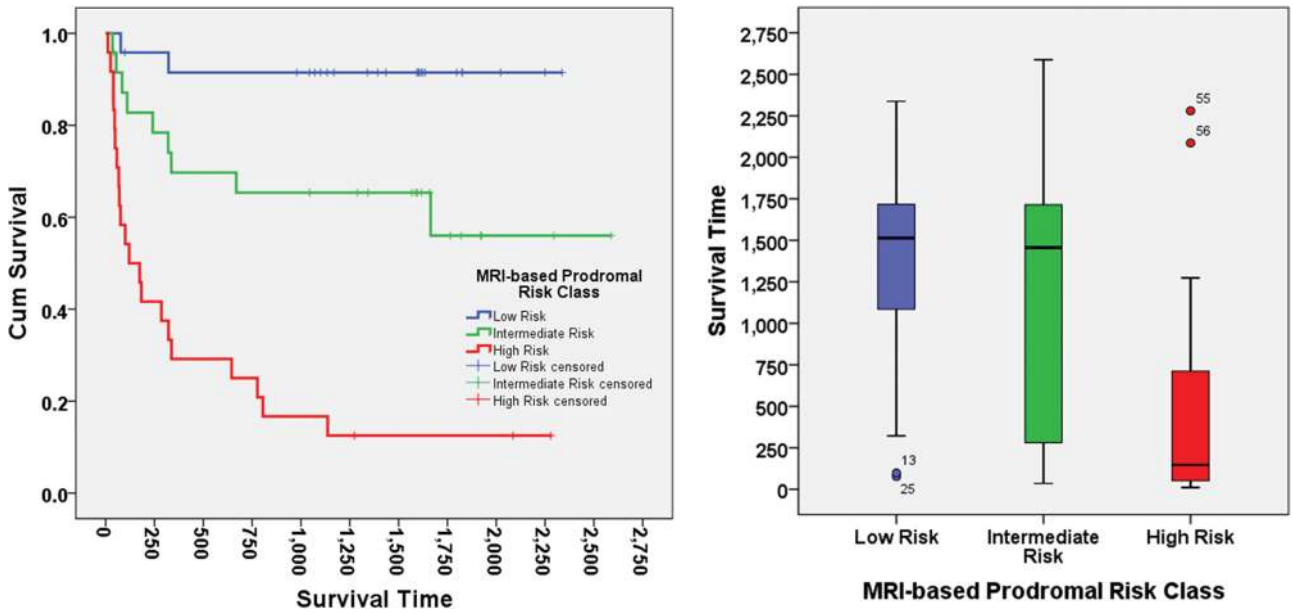

Fig. 2. (Left) Comparison of Kaplan-Meier survival curves in ARMS individuals with a low, intermediate, and high neuroanatomical risk level. Vertical lines indicate censoring events, while steps represent transition events in the ARMS population over the follow-up period. (Right) Box plot analysis of psychosis-free survival times across these three neuroanatomical risk levels. ARMS, at-risk mental states.

Table 3. Results of Kaplan-Meier Survival Analysis for Neuroanatomical Low-, Intermediate- and High-Risk Groups

Variable	Low Risk	Intermediate Risk	High Risk	$\chi 2$ (P)
Psychosis-free survival time: median (95% CI; range) [mo]	50.5 (37.4–54.0; 75.3)	48.5 (26.9–49.7; 85.1)	4.9 (6.2–24.3; 75.6)	*17.33 (<.001)*
Transition rate (95% CI) [%]	8.3 (3.3–30.8)	37.5 (21.1–57.4)	87.5 (68.2–97.3)	*29.04 (<.001)*
Pairwise log-rank tests [χ^2 (P)]				
Low risk	—	*5.38 (.020)*	*31.60 (<.001)*	—
Intermediate risk	*5.38 (0.020)*	—	*12.96 (<.001)*	—
Center composition of risk groups [N (%)]				
Munich	10 (40.0)	12 (50)	14 (58.3%)	1.65 (.469)
Basel	15 (60.0)	12 (50)	10 (41.7%)	

Note: Medians of psychosis-free survival times/transition rates were compared using median/chi-square tests. Pairwise difference between survival curves were evaluated by means of log-rank test. Finally, possible center × risk group interactions were assessed using the chi-square statistic. Italicized values indicate significant findings at an alpha level of 0.05.

ARMS had a transition rate of 87.5% and a median transition time of 147 days, whereas the respective values in the low-risk/intermediate-risk groups were 8.3%/37.5% and 1514 / 1456 days. Of the 8 (24.2%) misclassified ARMS-T subjects, 5 (63%)/3 (38%) were assigned to the intermediate-risk / low-risk groups. Risk groups did not significantly differ in their center composition (table 3).

The neuroanatomical decision function (figure 1) involved bilaterally reduced GM volume (−10%) in the prefrontal cortices of ARMS-T vs ARMS-NT subjects (table 4), covering the dorsomedial, ventromedial, and orbitofrontal areas and extending to the cingulate and right intra- and perisylvian structures (inferior frontal gyrus, Rolandic operculum, insula, temporal pole). Further subcortical GM reductions were detected in the right basal ganglia (11.3%), the vermal lobule 10 and the cerebellar lobules 7b, 8, Crus 1 and 2 (table 4). In contrast, increased GM volume in ARMS-T was found in (1) most right-hemispheric perisylvian and temporal structures (supramarginal, inferior parietal, angular cortex), and (2) subcortical structures including the right pallidum, the vermal lobules 6–9 and the cerebellar lobules 4, 5, 6, 9, and 10.

Discussion

This is, to the best of our knowledge, the first multicenter study aiming at identifying a single neuroanatomical surrogate of the psychosis prodrome *across* two independent high-risk cohorts. Our study extends previous single-center investigations[20,21,27,35] by pooling two independents high-risk cohorts recruited using *different* clinical high-risk criteria and examined by means of *different* MRI protocols. In summary, our main results suggest that the neuroanatomical signature of the prodrome may serve as an accurate biomarker to individually predict a high-risk person's clinical outcome in the early course of psychosis—in line with other neuropsychiatric conditions[36–39] and irrespective of between-site differences. Our supplementary analyses indicate that these differences can be effectively attenuated using post hoc statistical correction methods (Supplementary Analysis 1). Furthermore, we observed that prediction performance considerably depended on the available sample size (Supplementary Analysis 2), suggesting that the predictor's sensitivity and specificity will likely saturate in even larger training populations, as currently recruited across different international multicenter ARMS projects. Finally, we observed that this potential biomarker did not only predict a person's disease transition risk but also the time to transition. Both variables are of imminent importance for the *staging* of individual risk[40] and thus to the selection of optimal therapeutic interventions in the high-risk or prodromal phases of psychotic disorders.[41]

Neuroanatomy of Prodromal Psychosis

The visual analysis of the neuroanatomical predictor revealed GM volume reductions in ARMS-T vs ARMS-NT individuals covering prefrontal, cingulate, striatal, and cerebellar brain structures. Recent primate and large-scale human imaging studies suggest that these areas constitute prefronto-striato-cerebellar networks, which may subserve higher-order cognitive processes[42,43] and hence may underlie executive, reward-related, and mnemonic deficits in prodromal and established psychosis.[44–47] These findings overlap considerably with previous studies reporting GM volume reductions in the prefrontal, cingulate, perisylvian, and cerebellar cortices of genetic and clinical high-risk samples.[48] Furthermore, our results are in keeping with a series of neuroimaging studies that detected functional alterations of these networks in the ARMS, consisting of pathological associations between elevated striatal dopamine function and prefrontal activation during working memory and verbal fluency tasks.[10,48–50] These neurofunctional alterations seem to be

associated with the course of the ARMS, including both remission[51] and clinical deterioration.[52,53]

Interestingly, we also observed GM volume increments in ARMS-T vs ARMS-NT subjects, which showed a left temporal and inferior parietal distribution in line with findings reported by Borgwardt el al.[54] Given well-established progressive volume reductions in the temporo-parietal cortices of first-episode patients,[55] these intriguing relative GM volume increments in prodromal individuals have been interpreted in terms of a transient compensatory normalization of neural structure.[28,54,56] In this regard, the parallelism of volume decreases in the prefronto-striato-cerebellar network and relative volume increases in the left temporo-parietal cortex may point to a nonlinear disease process driving these complex neuroanatomical changes as the prodrome evolves into full-blown psychosis. Our work adds to this hypothesis by revealing that the predictive signature of the psychosis prodrome is homogeneously expressed at the single-subject level. Further longitudinal MRI studies are needed to map the neuroanatomical disease course and hence to pinpoint the position of our cross-sectional "snapshot" along the psychosis trajectory.

Evidence-based Risk Stratification Using Neuroanatomical Biomarkers

Recent reviews on early intervention in the ARMS have suggested that preventive therapy may reduce transition rates and improve outcomes through a variety of therapeutic strategies.[57] These promising results may be mediated through a better neurobiological responsiveness in the earliest phases of psychosis. In this regard, the accurate quantification of risk for further disease progression is a central diagnostic requirement in order to implement *stepped care*

Table 4. ROI Parcellation Analysis of Neuroanatomical Signature

Hemisphere	Left			Medial			Right			
Structure	K_{ROI}	Diff	SD	K_{ROI}	Diff	SD	K_{ROI}	Diff	SD	K_{ROI} [%]
Frontal	13.1	−10.5	5.3				14.7	−8.9	5.9	5
Frontal Inf Orb	8.8	−6.6	5.0				6.8	−9.7	4.3	10
Frontal Med Orb	7.9	−9.1	3.6				28.3	−10.1	3.7	15
Frontal Mid	10.1	−11.9	6.9				9.5	−6.7	10.4	20
Frontal Mid Orb	15.7	−8.7	3.5				15.0	−7.0	2.6	**25**
Frontal Sup	8.9	−18.8	11.8				8.1	−11.7	7.7	**30**
Frontal Sup Medial	15.6	−11.5	7.3				10.0	−7.7	4.7	
Frontal Sup Orb	21.8	−8.1	2.8				23.0	−7.1	2.0	
Rectus	17.5	−7.5	2.0				22.0	−9.4	4.6	
Supp Motor Area	11.2	−11.9	5.1				9.4	−10.4	13.0	
Temporal	6.2	5.2	9.1				8.5	5.6	7.8	
Fusiform	5.3	4.3	7.3							
Temporal Inf	5.5	4.0	10.2							
Temporal Mid	7.7	7.3	9.7				8.5	5.6	7.8	
Intra- and Perisylvian	8.3	2.6	10.2				12.0	−7.2	6.8	
Angular	13.0	7.0	9.1				6.7	−3.1	18.2	
Frontal Inf Oper	10.5	0.8	15.1				8.1	−7.8	3.1	
Frontal Inf Tri							19.9	−13.1	5.8	
Heschl							15.2	−5.1	1.3	
Insula	10.1	−3.0	5.9				15.6	−5.5	3.0	
Parietal Inf	7.1	6.9	15.1							
Rolandic Oper	5.5	−2.7	7.0				13.1	−7.7	5.6	
SupraMarginal	5.0	11.0	3.2							
Temporal Pole Sup	6.6	−1.9	16.4				5.3	−8.3	10.7	
Limbic	11.4	−6.3	5.8				7.6	−9.7	3.3	
Cingulum Ant	10.7	−8.5	4.2				10.2	−8.6	1.9	
Cingulum Mid	12.0	−4.2	7.5				7.6	−4.5	6.2	
Cingulum Post							5.1	−15.9	1.7	
Parietal	7.4	−0.4	12.1				5.2	4.2	10.6	
Parietal Sup	8.4	5.7	16.3				5.3	3.9	14.8	
Postcentral	7.4	−9.8	11.0							
Precuneus	6.4	2.9	9.0				5.1	4.5	6.4	
Occipital	6.6	1.8	13.2				10.9	−4.2	13.4	
Calcarine							11.5	−5.7	13.8	
Cuneus							8.2	−3.9	14.9	
Lingual							14.0	−7.7	13.3	
Occipital Inf	7.9	4.0	14.2				9.6	−4.4	9.7	
Occipital Sup	5.4	−0.4	12.2				11.2	0.5	15.4	

Table 4. Continued

Hemisphere	Left			Medial			Right			
Structure	K_{ROI}	Diff	SD	K_{ROI}	Diff	SD	K_{ROI}	Diff	SD	K_{ROI} [%]
Basal ganglia	9.2	1.8	8.3				21.4	−11.3	3.9	
Pallidum	9.1	8.4	11.0				18.8	−13.5	4.1	
Putamen	9.3	−4.8	5.6				24.0	−9.0	3.7	
Cerebellum	10.8	−5.1	9.6	10.8	2.9	1.9	12.0	−2.3	7.2	
Cerebellum 10							11.8	18.4	18.1	
Cerebellum 3							6.7	−9.6	6.0	
Cerebellum 4 5							8.4	7.1	4.3	
Cerebellum 6	13.6	5.1	2.4				14.9	5.8	3.7	
Cerebellum 7b	6.8	−10.6	16.6				11.4	−14.1	3.9	
Cerebellum 8	12.4	−5.3	9.8				6.4	−8.0	11.0	
Cerebellum 9	8.7	10.6	7.7				8.9	8.4	5.0	
Cerebellum Crus1	16.4	−15.7	12.6				25.0	−12.8	5.5	
Cerebellum Crus2	7.1	−15.0	8.5				14.2	−16.0	7.6	
Vermis 10				6.3	−13.6	0.0				
Vermis 6				12.5	4.0	1.9				
Vermis 7				12.0	5.7	1.6				
Vermis 8				13.8	9.0	1.8				
Vermis 9				9.5	9.5	4.2				

Note: Abbreviations: AAL, automated anatomical labeling; Ant, anterior; ARMS, at-risk mental states; Inf, inferior; Mid, middle; Orb, orbital; Oper, opercularis; Post, posterior; ROI, region of interest; Sup, superior; Supp, supplementary; Tri, triangularis. The table lists AAL-ROIs with >5% of their voxels having a probability >50% of reliably contributing to the average neuroanatomical decision boundary (see figure 1). Each ROI entry lists the percentage of suprathreshold voxels (K_{ROI}) and their mean (SD) volumetric difference (Diff) in ARMS-T vs ARMS-NT. Each entry was highlighted by a gray-scaled background, as defined by its K_{ROI}.

strategies in early intervention services.[58] Stepped care naturally embraces the Hippocratic precept of *primum nil nocere*, which in the case of early intervention consists of avoiding harmful treatment, unnecessary distress, and stigmatization due to false positive diagnostic labeling.[41]

In view of this precept, the established early recognition strategies identify persons at a 100-fold elevated risk of psychosis,[1] but this still does not allow deciding who necessitates intensive preventive efforts or, alternatively, who does not require any treatment at all. Thus, neurobiological and neurocognitive markers[4,6] in combination with clinical data[59,60] may ultimately enable the reliable single-subject quantification of risk *across different* early recognition centers. In turn, this progress will increase the safety and broader availability of early intervention. Our findings support the clinical applicability of such neurobiological markers in that we (1) detected a homogeneous neuroanatomical signature of emerging psychosis across *independent* high-risk cohorts and *despite* differing MRI data acquisition protocols, and (2) observed for the first time a close link between the ARMS persons' loadings on this MRI signature and their clinical risk level, as measured both in terms of transition likelihood and time to transition. Thus, given a baseline disease transition risk of 45% for an ARMS person over the next 4 years, a caregiver would have a 36%/26% higher prognostic certainty if this person receives a positive/negative MRI test result. Certainty would even further increase from 45% to 87% in a risk person having a MRI prediction score in the upper 33%-quantile. Hence, this prediction result would mark an imminent risk of disease transition, and as such a need for urgent preventive treatment. In contrast, for ARMS persons with an intermediate-to-low risk level a more conservative therapeutic approach would be indicated, which includes less harmful interventions like cognitive behavioral therapy to improve functioning, affective comorbidity[61] and prevent further deterioration, and regular reevaluations of the clinical and MRI status to monitor the development of risk markers over time. Importantly, for such evidence-based decision processes to operate in clinical reality, we will require an accurate biomarker that generalizes well to newly identified ARMS individuals, as suggested by our rigorous validation framework.

Challenges and Future Research Directions

Several challenges for future research efforts arise from our findings: First, the transition rate of 45% suggests a modestly higher (~10%) transition risk in our pooled population compared to other high-risk cohorts.[1] This increased risk may be caused by different pathways to care as our early recognition services are more linked with classical psychiatric institutions, whereas youth mental health services in Australia, the United States, or United Kingdom may enable persons to find professional help earlier and at lower thresholds. However, our ARMS cohort's transition risk was measured over an average follow-up period

of 4.4 years and thus overlaps with the risk range of other long-term investigations like the PACE-400[2] (35%; 95% CI: 29%–41%) or Cologne Early Recognition study (49%; 95% CI: 43%–57%).[3] Nevertheless, the generalization capacity of our candidate marker has to be further explored and validated in ARMS populations with a substantially lower risk of developing psychotic illness.

Second, the administration of the proposed MRI-based risk predictor requires the initial clinical exploration of a help-seeking person by specifically trained interviewers. This limits the broader availability of MRI-based risk prognostic tools across less specialized mental health services. A related issue in the present study is the use of checklists to assess the presence of prodromal symptoms (Supplementary Methods) followed by the application of BPRS/SANS and PANSS scales to evaluate symptom severity. As the initial clinical exploration represents an "upstream filter" to the MRI-based prognostic method, further prospective validation of our candidate marker is needed using current high-risk inventories. In this regard, the Schizophrenia Proneness Instrument,[62] the Structured Interview for Psychosis-Risk Syndromes,[63] or the Comprehensive Assessment of At-Risk Mental States[64] may provide more sensitive measures of prodromal symptomatology than scales developed for patients with established illness, and hence they may influence the performance of the downstream MRI predictor.

Third, profound between-center effects were detected that not only originated from scanner differences, but potentially also from heterogeneous ARMS inclusion criteria and a trend toward shorter transition intervals in the Munich sample. However, these supplementary data also suggest that such center effects can be effectively attenuated—as done in the present analysis—thus enabling the data pooling needed to create generalizable markers for the psychosis prodrome.

Finally, although our pattern recognition findings are based on a considerably larger ARMS sample compared to previous single-center studies,[20,21,27] it remains unclear whether these results will generalize to other ARMS cohorts examined using a wider variety of scanner variables (eg, different field strengths and MRI vendors). In this regard, our findings suggest that the performance of our candidate biomarker still lies on an ascending "learning curve," with the saturation point of its specificity and sensitivity to be reached at larger sample sizes, as recently shown for schizophrenia and Alzheimer's disease.[65,66] The good cross-center generalization capacity of MRI-based diagnostic tools demonstrated in these studies calls for the ultimate verification of our candidate marker in significantly larger samples, which will be provided by multicenter projects, like NAPLS 2,[67] EU-GEI,[68] PSYSCAN, and PRONIA (http://pronia.eu) over the next years. As only such large-scale data facilitate the rigorous evaluation of the biomarkers' out-of-center generalization capacity, they will allow to finally benchmarking the feasibility of MRI-enhanced early recognition and intervention in the psychosis prodrome.

Supplementary Material

Supplementary material is available at http://schizophreniabulletin.oxfordjournals.org.

Funding

The *FePsy* project was supported by the Swiss National Science Foundation [3200–057216.99, 3200-0572216.99, PBBSB-106936, 3232BO-119382]; the Nora van Meeuwen-Haefliger Stiftung, Basel (CH); and by unconditional grants from the Novartis Foundation, Bristol-Myers Squibb, GmbH (CH), Eli Lilly SA (CH), AstraZeneca AG (CH), Janssen-Cilag AG (CH), and Sanofi-Synthelabo AG (CH). The funding sources had no involvement in the study design, the collection and analysis of the data or the writing of the manuscript.

Acknowledgments

We would like to thank patients, coworkers of the *FePsy* and FETZ studies, especially Jacqueline Aston. The authors have declared that there are no conflicts of interest in relation to the subject of this study.

References

1. Fusar-Poli P, Bonoldi I, Yung AR, et al. Predicting psychosis: meta-analysis of transition outcomes in individuals at high clinical risk. *Arch Gen Psychiatry*. 2012;69:220–229.
2. Nelson B, Yuen HP, Wood SJ, et al. Long-term follow-up of a group at ultra high risk ("prodromal") for psychosis: the PACE 400 study. *JAMA Psychiatry*. 2013;70:793–802.
3. Klosterkötter J, Hellmich M, Steinmeyer EM, Schultze-Lutter F. Diagnosing schizophrenia in the initial prodromal phase. *Arch. Gen. Psychiatry*. 2001;58:158–164.
4. Koutsouleris N, Davatzikos C, Bottlender R, et al. Early recognition and disease prediction in the at-risk mental states for psychosis using neurocognitive pattern classification. *Schizophr Bull*. 2012;38:1200–1215.
5. Fusar-Poli P, Radua J, McGuire P, Borgwardt S. Neuroanatomical maps of psychosis onset: voxel-wise meta-analysis of antipsychotic-naive VBM studies. *Schizophr Bull*. 2012;38:1297–1307.
6. Bodatsch M, Ruhrmann S, Wagner M, et al. Prediction of psychosis by mismatch negativity. *Biol Psychiatry*. 2011;69:959–966.
7. Fusar-Poli P. Voxel-wise meta-analysis of fMRI studies in patients at clinical high risk for psychosis. *J Psychiatry Neurosci*. 2012;37:106–112.
8. Schmidt A, Smieskova R, Aston J, et al. Brain connectivity abnormalities predating the onset of psychosis: correlation with the effect of medication. *JAMA Psychiatry (Archives of General Psychiatry)*. *JAMA Psychiatry*. 2013;70:903–912.
9. Allen P, Chaddock CA, Howes OD, et al. Abnormal relationship between medial temporal lobe and subcortical dopamine function in people with an ultra high risk for psychosis. *Schizophr Bull*. 2012;38:1040–1049.
10. Fusar-Poli P, Broome MR, Matthiasson P, et al. Prefrontal function at presentation directly related to clinical outcome

in people at ultrahigh risk of psychosis. *Schizophr Bull*. 2011;37:189–198.

11. Fusar-Poli P, Perez J, Broome M, et al. Neurofunctional correlates of vulnerability to psychosis: a systematic review and meta-analysis. *Neurosci Biobehav Rev*. 2007;31:465–484.
12. Smieskova R, Fusar-Poli P, Allen P, et al. Neuroimaging predictors of transition to psychosis–a systematic review and meta-analysis. *Neurosci Biobehav Rev*. 2010;34:1207–1222.
13. Fusar-Poli P, Radua J, Frascarelli M, et al. Evidence of reporting biases in voxel-based morphometry (VBM) studies of psychiatric and neurological disorders [published online ahead of print October 07, 2013]. *Hum Brain Mapp*. doi: 10.1002/hbm.22384.
14. Davatzikos C. Why voxel-based morphometric analysis should be used with great caution when characterizing group differences. *Neuroimage*. 2004;23:17–20.
15. Friston KJ, Ashburner J. Generative and recognition models for neuroanatomy. *Neuroimage*. 2004;23:21–24.
16. Vapnik VN. An overview of statistical learning theory. *IEEE Trans. Neural Netw*. 1999;10:988–999.
17. Klöppel S, Abdulkadir A, Jack CR Jr, Koutsouleris N, Mourao-Miranda J, Vemuri P. Diagnostic neuroimaging across diseases. *Neuroimage*. 2012;61:457–463.
18. Orrù G, Pettersson-Yeo W, Marquand AF, Sartori G, Mechelli A. Using support vector machine to identify imaging biomarkers of neurological and psychiatric disease: a critical review. *Neurosci Biobehav Rev*. 2012;36:1140–1152.
19. Lao Z, Shen D, Xue Z, Karacali B, Resnick SM, Davatzikos C. Morphological classification of brains via high-dimensional shape transformations and machine learning methods. *Neuroimage*. 2004;21:46–57.
20. Koutsouleris N, Borgwardt S, Meisenzahl EM, Bottlender R, Möller H-J, Riecher-Rössler A. Disease prediction in the at-risk mental state for psychosis using neuroanatomical biomarkers: results from the FePsy study. *Schizophr Bull*. 2012;38:1234–1246.
21. Koutsouleris N, Meisenzahl EM, Davatzikos C, et al. Use of neuroanatomical pattern classification to identify subjects in at-risk mental states of psychosis and predict disease transition. *Arch Gen Psychiatry*. 2009;66:700–712.
22. Phillips KA, Van Bebber S, Issa AM. Diagnostics and biomarker development: priming the pipeline. *Nat Rev Drug Discov*. 2006;5:463–469.
23. Riecher-Rössler A, Gschwandtner U, Aston J, et al. The Basel early-detection-of-psychosis (FEPSY)-study–design and preliminary results. *Acta Psychiatr Scand*. 2007;115:114–125.
24. Morrison AP, French P, Walford L, et al. Cognitive therapy for the prevention of psychosis in people at ultra-high risk: randomised controlled trial. *Br J Psychiatry*. 2004;185:291–297.
25. Yung AR, Phillips LJ, McGorry PD, et al. Prediction of psychosis. A step towards indicated prevention of schizophrenia. *Br J Psychiatry Suppl*. 1998;172:14–20.
26. McGuffin P, Farmer A, Harvey I. A polydiagnostic application of operational criteria in studies of psychotic illness. Development and reliability of the OPCRIT system. *Arch Gen Psychiatry*. 1991;48:764–770.
27. Borgwardt S, Koutsouleris N, Aston J, et al. Distinguishing prodromal from first-episode psychosis using neuroanatomical single-subject pattern recognition. *Schizophr Bull*. 2013;39:1105–1114.
28. Koutsouleris N, Schmitt G, Gaser C, et al. Neuroanatomical correlates of different vulnerability states of psychosis in relation to clinical outcome. *Br J Psychiatry*. 2009;195:218–226.
29. Filzmoser P, Liebmann B, Varmuza K. Repeated double cross validation. *J Chemometrics*. 2009;23:160–171.
30. Sun Y, Todorovic S, Goodison S. Local learning based feature selection for high dimensional data analysis. *IEEE Trans Pattern Anal Mach Intell*. 2010;32:1610–1626.
31. Hubert M, Rousseeuw P, Verdonck T. Robust PCA for skewed data and its outlier map. *Computational Statistics & Data Analysis*. 2009;53:2264–2274.
32. Schölkopf B, Smola A, Williamson RC, Bartlett PL. New support vector algorithms. *Neural Computation*. 2000;12:1207–1245.
33. Schmahmann JD, Doyon J, McDonald D, et al. Three-dimensional MRI atlas of the human cerebellum in proportional stereotaxic space. *Neuroimage*. 1999;10:233–260.
34. Tzourio-Mazoyer N, Landeau B, Papathanassiou D, et al. Automated anatomical labeling of activations in SPM using a macroscopic anatomical parcellation of the MNI MRI single-subject brain. *Neuroimage*. 2002;15:273–289.
35. Pettersson-Yeo W, Benetti S, Marquand AF, et al. Using genetic, cognitive and multi-modal neuroimaging data to identify ultra-high-risk and first-episode psychosis at the individual level. *Psychol Med*. 2013;43:2547–2562.
36. Bendfeldt K, Klöppel S, Nichols TE, et al. Multivariate pattern classification of gray matter pathology in multiple sclerosis. *Neuroimage*. 2012;60:400–408.
37. Davatzikos C, Bhatt P, Shaw LM, Batmanghelich KN, Trojanowski JQ. Prediction of MCI to AD conversion, via MRI, CSF biomarkers, and pattern classification. *Neurobiol Aging*. 2011;32:2322.e19–2322.e27.
38. Klöppel S, Chu C, Tan GC, et al. Automatic detection of preclinical neurodegeneration: presymptomatic Huntington disease. *Neurology*. 2009;72:426–431.
39. Mourao-Miranda J, Reinders AATS, Rocha-Rego V, et al. Individualized prediction of illness course at the first psychotic episode: a support vector machine MRI study. *Psychol Med*. 2012;42:1037–1047.
40. Wood SJ, Yung AR, McGorry PD, Pantelis C. Neuroimaging and treatment evidence for clinical staging in psychotic disorders: from the at-risk mental state to chronic schizophrenia. *Biol Psychiatry*. 2011;70:619–625.
41. Ruhrmann S, Klosterkötter J, Bodatsch M, et al. Chances and risks of predicting psychosis. *Eur Arch Psychiatry Clin Neurosci*. 2012;262(suppl 2):85–90.
42. Bostan AC, Dum RP, Strick PL. The basal ganglia communicate with the cerebellum. *Proc Natl Acad Sci U S A*. 2010;107:8452–8456.
43. Buckner RL, Krienen FM, Castellanos A, Diaz JC, Yeo BTT. The organization of the human cerebellum estimated by intrinsic functional connectivity. *J Neurophysiol*. 2011;106:2322–2345.
44. Allen P, Luigjes J, Howes OD, et al. Transition to psychosis associated with prefrontal and subcortical dysfunction in ultra high-risk individuals. *Schizophr Bull*. 2012; 38:1268–1276.
45. Fusar-Poli P, Deste G, Smieskova R, et al. Cognitive functioning in prodromal psychosis: a meta-analysis. *Arch Gen Psychiatry*. 2012;69:562–571.
46. Koutsouleris N, Gaser C, Patschurek-Kliche K, et al. Multivariate patterns of brain-cognition associations relating to vulnerability and clinical outcome in the at-risk mental states for psychosis. *Hum Brain Mapp*. 2012;33:2104–2124.
47. Koutsouleris N, Patschurek-Kliche K, Scheuerecker J, et al. Neuroanatomical correlates of executive dysfunction

in the at-risk mental state for psychosis. *Schizophr Res*. 2010;123:160–174.

48. Smieskova R, Marmy J, Schmidt A, et al. Do subjects at clinical high risk for psychosis differ from those with a genetic high risk?—a systematic review of structural and functional brain abnormalities. *Curr Med Chem*. 2013;20:467–481.
49. Fusar-Poli P, Howes OD, Allen P, et al. Abnormal frontostriatal interactions in people with prodromal signs of psychosis: a multimodal imaging study. *Arch Gen Psychiatry*. 2010;67:683–691.
50. Fusar-Poli P, Howes OD, Allen P, et al. Abnormal prefrontal activation directly related to pre-synaptic striatal dopamine dysfunction in people at clinical high risk for psychosis. *Mol Psychiatry*. 2011;16:67–75.
51. Fusar-Poli P, Broome MR, Matthiasson P, et al. Prefrontal function at presentation directly related to clinical outcome in people at ultrahigh risk of psychosis. *Schizophr Bull*. 2011;37:189–198.
52. Howes O, Bose S, Turkheimer F, et al. Progressive increase in striatal dopamine synthesis capacity as patients develop psychosis: a PET study. *Mol Psychiatry*. 2011;16:885–886.
53. Morey RA, Inan S, Mitchell TV, Perkins DO, Lieberman JA, Belger A. Imaging frontostriatal function in ultra-high-risk, early, and chronic schizophrenia during executive processing. *Arch Gen Psychiatry*. 2005;62:254–262.
54. Borgwardt SJ, Riecher-Rössler A, Dazzan P, et al. Regional gray matter volume abnormalities in the at risk mental state. *Biol Psychiatry*. 2007;61:1148–1156.
55. Vita A, De Peri L, Deste G, Sacchetti E. Progressive loss of cortical gray matter in schizophrenia: a meta-analysis and meta-regression of longitudinal MRI studies. *Transl Psychiatry*. 2012;2:e190.
56. Phillips LJ, Velakoulis D, Pantelis C, et al. Non-reduction in hippocampal volume is associated with higher risk of psychosis. *Schizophr Res*. 2002;58:145–158.
57. Preti A, Cella M. Randomized-controlled trials in people at ultra high risk of psychosis: a review of treatment effectiveness. *Schizophr Res*. 2010;123:30–36.
58. Francey SM, Nelson B, Thompson A, et al. Who needs antipsychotic medication in the earliest stages of psychosis? A reconsideration of benefits, risks, neurobiology and ethics in the era of early intervention. *Schizophr Res*. 2010;119:1–10.
59. Michel C, Ruhrmann S, Schimmelmann BG, Klosterkötter J, Schultze-Lutter F. A stratified model for psychosis prediction in clinical practice [published online ahead of print March 07, 2014]. *Schizophr Bull*. doi:10.1093/schbul/sbu025
60. Riecher-Rössler A, Pflueger MO, Aston J, et al. Efficacy of using cognitive status in predicting psychosis: a 7-year follow-up. *Biol Psychiatry*. 2009;66:1023–1030.
61. Fusar-Poli P, Nelson B, Valmaggia L, Yung AR, McGuire PK. Comorbid depressive and anxiety disorders in 509 individuals with an at-risk mental state: impact on psychopathology and transition to psychosis. *Schizophr Bull*. 2014;40:120–131.
62. Schultze-Lutter F, Addington J, Ruhrmann S, Klosterkötter J. *Schizophrenia Proneness Instrument, Adult Version (SPI-A)*. Rome, Italy: Giovanni Fioriti Editore; 2007.
63. Miller TJ, McGlashan TH, Rosen JL, et al. Prodromal assessment with the structured interview for prodromal syndromes and the scale of prodromal symptoms: predictive validity, interrater reliability, and training to reliability. *Schizophr Bull*. 2003;29:703–715.
64. Yung AR, Yuen HP, McGorry PD, et al. Mapping the onset of psychosis: the comprehensive assessment of at-risk mental states. *Aust N Z J Psychiatry*. 2005;39:964–971.
65. Abdulkadir A, Mortamet B, Vemuri P, et al. Effects of hardware heterogeneity on the performance of SVM Alzheimer's disease classifier. *Neuroimage*. 2011.
66. Nieuwenhuis M, van Haren NEM, Hulshoff Pol HE, Cahn W, Kahn RS, Schnack HG. Classification of schizophrenia patients and healthy controls from structural MRI scans in two large independent samples. *Neuroimage*. 2012;61:606–612.
67. Addington J, Cadenhead KS, Cornblatt BA, et al. North American Prodrome Longitudinal Study (NAPLS 2): overview and recruitment. *Schizophr Res*. 2012;142:77–82.
68. van Os J, Rutten BP, Poulton R. Gene-environment interactions in schizophrenia: review of epidemiological findings and future directions. *Schizophr Bull*. 2008;34:1066–1082.